

# Unique Ultrastructural Alterations in the Placenta Associated With Macrosomia Induced by Gestational Diabetes Mellitus

Junxiang Wei<sup>1</sup>, Tianyu Dong<sup>1</sup>, Mingxia Chen<sup>2</sup>, Xiao Luo<sup>3</sup>, Yang Mi<sup>1,\*</sup>

## Abstract

**Objective:** To investigate the morphological and ultrastructural alterations in placentas from pregnancies with gestational diabetes mellitus (GDM)-induced macrosomia, term nondiabetic macrosomia, and normal pregnancies.

**Methods:** Sixty full-term placentas were collected, and clinical data along with informed consent were obtained from pregnant women who underwent regular visit checks and delivered their newborns in Northwest Women's and Children's Hospital between May and December 2022. Placentas were divided into three equal groups: normal pregnancy (control group), nondiabetic macrosomia group, and macrosomia complicated with GDM (diabetic macrosomia) group. Gross morphological data of placentas were recorded, and placental samples were processed for examination of ultrastructural and stereological changes using transmission electron microscopy. Analysis of variance and chi-squared test were used to examine the differences among the three groups for continuous and categorical variables, respectively.

**Results:** The baseline characteristics of mothers and neonates did not differ across the three groups, except for a significantly higher birth weight in the diabetic macrosomia group ( $4172.00 \pm 151.20$  g vs.  $3192.00 \pm 328.70$  g,  $P < 0.001$ ) and nondiabetic macrosomia group ( $4138.00 \pm 115.20$  g vs.  $3192.00 \pm 328.70$  g,  $P < 0.001$ ) compared with control group. Examination of the placentas revealed that placental weight was also highest in the diabetic macrosomia group compared with control group ( $810.00 \pm 15.81$  g vs.  $490.00 \pm 51.48$  g,  $P < 0.001$ ) and nondiabetic macrosomia group ( $810.00 \pm 15.81$  g vs.  $684.00 \pm 62.69$  g,  $P < 0.001$ ), but the ratio of neonatal birth weight to placental weight (BW/PW) was significantly lower in the diabetic macrosomia group compared with that in the control group ( $5.15 \pm 0.19$  vs.  $6.54 \pm 0.63$ ,  $P < 0.001$ ) and nondiabetic macrosomia group ( $5.15 \pm 0.19$  vs.  $6.09 \pm 0.52$ ,  $P < 0.001$ ) group. In contrast, the BW/PW ratio in nondiabetic macrosomia did not differ significantly from that in the control group. Distinct ultrastructural changes in terminal villi and stereological alterations in microvilli were observed in the diabetic macrosomia group, including changes in the appearance of cytoplasmic organelles and the fetal capillary endothelium and thickness of the vasculo-syncytial membrane and basal membrane.

**Conclusion:** Significant ultrastructural and stereological alterations were discovered in the placentas from pregnant women with macrosomia induced by GDM. These alterations may be the response of the placenta to the hyperglycemia condition encountered during pregnancies complicated with GDM.

**Keywords:** Placenta; Macrosomia; Gestational diabetes mellitus; Ultrastructure; Morphology

## Introduction

Gestational diabetes mellitus (GDM) is a serious pregnancy complication characterized by abnormal glucose tolerance that occurs or is first recognized during pregnancy.<sup>1</sup> GDM affects approximately 14.0% of pregnancies globally,<sup>2</sup> with

a prevalence of 14.8% among pregnant women in China.<sup>3</sup> These numbers are increasing owing to the rising obesity epidemic. GDM has a significant effect on maternal and infant health. For example, GDM is associated with various placenta-mediated obstetric complications, particularly fetal macrosomia, which is a condition where the neonatal birth weight is larger than 4000 g. Studies have indicated that approximately 15%–45% of newborns born to diabetic mothers can have macrosomia, compared with 12% of newborns born to nondiabetic mothers.<sup>4</sup> The occurrence of macrosomia at birth elevates the risk of complications such as shoulder dystocia, clavicle fractures, and brachial plexus injury in infants, as well as cesarean delivery, postpartum hemorrhage, and vaginal lacerations in mothers,<sup>5</sup> thus posing a significant threat to the health of mothers and infants.

The placenta acts as a critical interface between the mother and fetus, performing a wide range of endocrine and transport functions. Connecting the maternal and fetal blood circulations, the placenta facilitates the exchange of nutrients, respiratory gases, and waste products between mother and fetus.<sup>6</sup> Furthermore, the placenta is influenced by maternal and/or fetal metabolic changes, making it a target organ for such alterations.<sup>7</sup> The placenta adapts to the varying maternal-fetal environment during different stages of pregnancy and in the

<sup>1</sup>Department of Obstetrics, Northwest Women's and Children's Hospital, Xi'an 710061, China; <sup>2</sup>Laboratory of Electron Microscope, Health Science Center of Xi'an Jiaotong University, Xi'an 710049, China; <sup>3</sup>Department of Physiology and Pathophysiology, School of Basic Medical Sciences, Health Science Center of Xi'an Jiaotong University, Xi'an 710049, China.

\* Corresponding author: Yang Mi, Department of Obstetrics, Northwest Women's and Children's Hospital, Xi'an 710061, China.  
E-mail: miyangmm@163.com

Copyright © 2024 The Chinese Medical Association, published by Wolters Kluwer Health, Inc.

This is an open-access article distributed under the terms of the Creative Commons Attribution-Non Commercial-No Derivatives License 4.0 (CCBY-NC-ND), where it is permissible to download and share the work provided it is properly cited. The work cannot be changed in any way or used commercially without permission from the journal.

Maternal-Fetal Medicine (2024) 6:3

Received: 14 August 2023 / Accepted: 10 April 2024

First online publication: 1 July 2024

<http://dx.doi.org/10.1097/FM9.0000000000000240>

presence of certain pathologies, ensuring optimal fetal growth and development.<sup>8</sup> However, excessive deviations, such as exposure to a complicated pregnancy involving GDM or an overnutritional environment, can affect the development and function of the placenta. Such deviations can cause ultrastructure alterations and abnormalities in the placental exchange barrier, particularly in the vasculo-syncytial membrane (VSM). The VSM is crucial for maintaining the exchange surface area between the maternal and fetal surfaces. Therefore, any alteration or dysfunction of this placental barrier reduces the area available for exchange, resulting in disrupted fetal growth and function. For example, human and experimental models showed that mice fed on a diet containing high levels of sugar and/or fat had increased barrier thickness in association with reduced fetal birth weight.<sup>9–11</sup> Another study revealed that hyperglycemia and hypoxia exposure in pregnancy caused placental malformation and decreased placental efficiency, which contribute to suboptimal fetal outcomes in offspring.<sup>12</sup> Therefore, abundant evidence indicates that alterations in placental structures affect placental function and fetal development.

Hyperglycemia induces oxidative stress in the GDM-complicated placenta, which can adversely affect the structure and function of the placenta during critical periods of placental development. In this study, we aimed to investigate the relationship between placental functions and fetal origin diseases by examining the morphology and ultrastructure alterations in human placentas of GDM-induced macrosomia and non-GDM-induced macrosomia using transmission electron microscopy.

## Materials and methods

### Study participants and design

All pregnant women who underwent regular visit checks and delivered their newborns at the Department of Obstetrics and Gynecology in Northwest Women's and Children's Hospital between May and December 2022 were invited to participate in the study. The inclusion criteria were as follows: pregnant women who reached full term defined as completing 37 weeks of gestation, with singleton pregnancies, and delivered via cesarean section. Exclusion criteria included the following: pregnant women with other pregnancy complications and medical disorders other than GDM; women with a history of pregestational diabetes; use of any antidiabetic drugs during pregnancy; and those with a nonsingleton pregnancy. Clinical information of eligible women, including maternal age, gestational weeks at delivery, pregestational weight and height, gestational weight gain, neonate birth weight, and sex, was collected and recorded. Sixty placentas were collected from eligible subjects and divided into three groups. Group I (control group) included 20 placentas from normal pregnancies, group II included 20 placentas from nondiabetic macrosomia cases, and group III contained 20 placentas from GDM type A2-induced macrosomia cases.

### Measurements and assessment

A 75-g oral glucose tolerance test was conducted on women at 24–28 weeks of gestation who were not previously diagnosed with overt diabetes. Plasma glucose levels were measured while fasting and at 1 and 2 h after the glucose intake. The diagnosis of GDM was established if any of the following

criteria, based on the American Diabetes Association (2011) guidelines,<sup>13</sup> were met: fasting glucose  $\geq 5.1$  mmol/L (92 mg/dL), 1 h  $\geq 10.0$  mmol/L (180 mg/dL), 2 h  $\geq 8.5$  mmol/L (153 mg/dL). Macrosomia was defined as a birth weight  $>4000$  g. The gross morphology of the placenta was assessed, and the following parameters were examined and recorded: placental weight, placental volume, placental thickness, and neonatal birth weight. Placental weight was measured using a digital scale of 0.01 g precision. Placental thickness was measured using a digital caliper with 0.01-mm precision in three points and taking the mean for estimation of the total placental volume. The placental surface area was determined by the formula of  $A = \Sigma P \times A(p)$ , where  $\Sigma P$  is the sum of the number of points landing on the surface of the placenta, and  $A(p)$  is the area associated with each point in the stereological grid. The total volume of each placenta was then estimated using the formula  $V = A \times t$ , where  $V$  is placental volume,  $A$  is placental surface area, and  $t$  is the mean thickness of the placenta.<sup>14</sup> Terminal villi were evaluated to assess aspects of the placental blood barrier, including the thickness of the syncytiotrophoblast basement membrane (BM) and fetal capillary BM.

### Placental sample collection

Immediately after labor, placental tissue samples were collected from the central part of the placenta. First, 2–3 blocks of specimens, each measuring  $0.5 \text{ cm}^3$  were collected and placed in ice-cold phosphate-buffered saline. The samples were then cleaned of blood and promptly cut into fragments of  $1 \text{ mm}^3$ . These fragments were fixed with 2.5% glutaraldehyde at  $4^\circ \text{C}$  before further processing for transmission electron microscopy (TEM) examination. To minimize the variations among villous structures, tissue blocks were collected from four different sites of the placenta, and two blocks from each placenta were randomly selected for examination.

### TEM processing and examination

Placental samples for the three groups were prepared and subjected to TEM examination at the TEM laboratory of Xi'an Jiaotong University Health Science Centre, with the aim of observing ultrastructural changes in the placentas.

The placental samples were initially fixed in a solution containing 2.5% glutaraldehyde and osmium tetroxide. Subsequently, they were dehydrated using alcohol and embedded in an epoxy resin. The sections were prepared using an ultramicrotome of approximately  $1\text{--}2 \mu\text{m}$  in thickness, and these sections were stained with Meilan and examined using an Olympus light microscope. Ultrathin sections, approximately  $0.05 \mu\text{m}$  thick, were then prepared and stained with uranyl acetate and lead citrate. These sections were systematically examined using a transmission electron microscope (Hitachi HT-7650, Japan) at various magnifications. For each tissue section, five randomly selected fields of vision were examined at magnifications of  $\times 4000$ ,  $\times 10,000$ ,  $\times 30,000$ , and  $\times 50,000$ . The fields of vision for each tissue block were nonoverlapping and different. Stereological analysis was performed using images captured at different magnifications and transferred to a computer using a digital photomicroscope. The stereological grid containing organized points was superimposed on the tissue images, and the stereological parameters including volume, surface density, and shape and distribution of placenta

microvilli and intervillous space were estimated using a computerized stereology program (Image Pro). Volume density for placenta microvilli and intervillous space was estimated as part of the analysis of 3D spatial arrangements using the point counting principle, and surface density was determined by intersection counting. The thickness of VSM was measured from intervillous space to the fetal vessels; the fetal capillary BM was measured between the syncytiotrophoblast and fetal endothelium BM under  $\times 50,000$  magnification using the TEM Image Platform. To eliminate bias, two operators independently performed the microscopic examinations and were unaware of the placental groups being examined.

Statistical analysis

The data were presented as the mean and standard deviation or median (interquartile range) for quantitative data and as the number and percentage (%) for qualitative data. Statistical differences among more than two groups were assessed using a one-way analysis of variances test for normal distributed continuous variables, whereas the nonparametric test of Kruskal-Wallis test was used for nonnormal distributed continuous variables; the least significant difference was used for pairwise comparison between groups. The chi-squared test was used for the differences test for categorical variables. All statistical analyses were performed using SPSS software (version 22.0 for Windows). A two-sided  $P$  value  $<0.05$  was considered statistically significant when interpreting all results.

Ethical approval

All participants were informed about the study details, and written informed consent for research use of placental samples was obtained prior to labor. This study was approved by the institutional ethical committee at Northwest Women’s and Children’s Hospital (no. 2-23-059).

Results

Clinical characteristics of study participants

The clinical data on mothers and neonates are summarized in Table 1. There were no significant differences in maternal

age, gravidity, gestational weeks at delivery, preconception body mass index (BMI), and gestational weight gain among mothers with macrosomia, macrosomia induced by GDM, and normal pregnancy. However, the neonatal birth weight was significantly higher in the GDM with macrosomia group compared with the control group ( $P < 0.001$ ).

Gross morphological assessment of the placenta

Table 2 presents the mean placental weight, placental volume, and the ratio of neonatal birth weight to placental weight (BW/PW) for normal pregnancy, macrosomia, and GDM with macrosomia. Significant differences were observed in these gross placental morphological parameters such as placental weight and BW/PW ratio among the three groups. Specifically, placentas from GDM with macrosomia exhibited the highest placental weight and neonatal birth weight compared with those of the other two groups, but the BW/PW was the lowest in the diabetic macrosomia group ( $P = 0.002$ ).

Ultrastructural changes in terminal villi from TEM

The control group exhibited normal morphology and thickness of the VSM, which consisted of a monolayer of syncytiotrophoblasts with multiple nuclei and abundant apical microvilli facing the intervillous space (Fig. 1A). The syncytiotrophoblasts formed a continuous syncytial layer, whereas the cytotrophoblasts were scattered beneath the syncytium (Fig. 1B). In the group with macrosomia placentas, the VSM thickness was nearly normal and comprised a single layer of syncytiotrophoblastic cells (Fig. 1C). The microvilli appeared normal in this group in terms of orientation, number, and size, but some abnormalities were observed, such as shortened, blunt microvilli with reduced numbers per micron (Fig. 1D). In group III (macrosomia with maternal GDM), the VSM was abnormally thick and uneven (Fig. 1E). In addition, the microvilli of the syncytiotrophoblasts in this group were significantly reduced in number and appeared shorter, scanty, and distorted (Fig. 1F).

In the control group, cytoplasmic organelles such as mitochondria, endoplasmic reticulum (ER), free ribosomes, and Golgi apparatus (GA) were clearly visible (Fig. 2A). The

**Table 1**  
Clinical characteristics of mothers and neonates in the three groups.

Characteristic	Control group ( <i>n</i> = 20)	Nondiabetic macrosomia group ( <i>n</i> = 20)	Diabetic macrosomia group ( <i>n</i> = 20)	Statistical values	<i>P</i>
Maternal age (years)	31.00 ± 2.24	29.80 ± 1.30	30.40 ± 4.83	0.180*	0.837
Gestational age at delivery (weeks)	39.28 ± 0.20	39.71 ± 0.23	39.68 ± 0.57	2.086*	0.160
Gravidity	2.0 (1.0–2.0)	1.0 (1.0–2.0)	1.0 (1.0–1.5)	2.971†	0.108
Pregestational BMI (kg/m <sup>2</sup> )	22.19 ± 4.74	22.88 ± 4.47	23.64 ± 3.89	0.118*	0.386
Gain weight (kg)	16.60 ± 2.97	14.90 ± 3.05	14.50 ± 3.61	0.600*	0.565
Neonatal birth weight (g)	3192.00 ± 328.70	4138.00 ± 115.20	4172.00 ± 151.20	32.195*	<0.001§
Infant sex				<0.001‡	>0.999
Male	10 (50)	12 (60)	11 (55)		
Female	10 (50)	8 (40)	9 (45)		

Data are presented as mean ± standard deviation, median (interquartile range), or *n* (%).

\**t* values.

†*Z* value.

‡Chi-squared value.

§Neonatal birth weight (g) significantly differed between the control group and both the nondiabetic and diabetic macrosomia groups.

BMI: Body mass index.



**Table 2**  
**Gross morphological characteristics of placenta in the three groups.**

Characteristic	Control group (n = 20)	Nondiabetic macrosomia group (n = 20)	Diabetic macrosomia group (n = 20)	Statistical values	P
Placental weight (g)	490.00 ± 51.48	684.00 ± 62.69	810.00 ± 15.81	32.632*	<0.001 <sup>‡</sup>
Placental volume (mL)	19.20 (19.19–19.72)	21.21 (18.19–21.23)	20.20 (19.23–23.25)	1.102 <sup>†</sup>	0.260
Placental thickness (mm)	31.31 ± 2.78	33.12 ± 3.15	34.83 ± 4.39	2.195*	0.110
BW/PW	6.54 ± 0.63	6.09 ± 0.52	5.15 ± 0.19	10.720*	0.002 <sup>§</sup>

Data are presented as mean ± standard deviation or median (interquartile range).  
\*t values.  
<sup>†</sup>Z value.  
<sup>‡</sup>The three groups all showed significant differences from each other in the placental weight (g).  
<sup>§</sup>BW/PW significantly differed between the diabetic macrosomia group and both the control and nondiabetic groups.  
BW/PW: Birthweight to placental weight ratio.

mitochondria were typically round or oval with well-developed cristae, and free ribosomes were dispersed throughout the cytoplasm. The rough ER was distributed around the mitochondria (Fig. 2B). In group II (nondiabetic macrosomia), reductions in mitochondrial numbers and rough ER were observed (Fig. 2C), and the mitochondria appeared slightly swollen (Fig. 2D). Group III (macrosomia with maternal GDM) contained a significant presence of swollen or even destroyed mitochondria, characterized by loss of cristae, and abundant dilated rough ER (Fig. 2E&F).

In the control group, the nuclear chromatin exhibited a fine dispersed pattern with abundant euchromatin (Fig. 3A). The BM of the fetal endothelium appeared continuous, uniform, and had a thin basal lamina that was similar to the BM of syncytiotrophoblasts. The luminal surface of the fetal capillary had a smooth appearance (Fig. 3B). In the nondiabetic macrosomia group, condensed hyperchromatic nuclei with a normal, intact, single-layered nuclear membrane were observed (Fig. 3C). The BM thickness was regular, and the luminal surface of the vascular endothelium was relatively smooth (Fig. 3D). In group III (macrosomia with maternal GDM), the nuclei displayed folded, double-layered, edematous nuclear membranes, and the chromatin appeared as dense peripheral clumps (Fig. 3E). In addition, the villous vessels in this group exhibited abnormalities such as endothelial cell folding, resulting in the luminal surfaces protruding into the vascular lumen and causing a narrower caliber (Fig. 3F).

**Stereological change in the apical microvilli from TEM of the placenta**

The volume density, surface density, and shape of apical microvilli were significantly reduced in diabetic macrosomia compared to the control group and nondiabetic macrosomia, while the distribution of microvilli was significantly higher than that in the control and nondiabetic macrosomia groups. In addition, the BMs of syncytiotrophoblasts and the fetal capillary were significantly thicker in the diabetic macrosomia group compared to the control group and nondiabetic macrosomia ( $P < 0.001$ ) (Table 3).

**Discussion**

The placenta, a complex organ consisting of various cell types with different origins, responds to maternal environmental changes or stress in an attempt to maintain fetal viability. In this study, we observed significant morphological and ultra-

structural changes in the placenta of diabetic macrosomia cases. These changes included a decreased BW/PW ratio and a decreased density of syncytiotrophoblast apical microvilli. These alterations likely contribute to the inhibition of transplacental transport and exchange.

Placentas from pregnancies with GDM have been reported to be heavier and larger than those from normal pregnancies.<sup>15,16</sup> Previous studies have also indicated a linear correlation among placental weight, placental volume, and birth weight.<sup>17,18</sup> In our study, we observed that placentas from diabetic macrosomia cases were significantly heavier compared with those from nondiabetic macrosomia and normal pregnancies. Furthermore, placentas from nondiabetic macrosomia cases were also heavier than those from normal pregnancies. Besides heavier placentas, various changes including inflammation, DNA methylation, and altered expression of genes regulating metabolism and angiogenesis occur in the placenta under a diabetic environment.<sup>19</sup> The structural and functional alterations induced by hyperglycemia exposure in pregnancy have been reported to insignificantly increase the risk of adverse offspring pregnancy outcomes.<sup>20</sup> In addition, our findings showed that the birth weight of infants from diabetic macrosomia cases was significantly higher compared with that of nondiabetic and normal pregnancies. The BW/PW ratio is commonly used as an indicator of placental efficiency and is defined as the grams of fetus produced per gram of placenta.<sup>21</sup> Our results indicated a significantly lower BW/PW ratio in pregnancies with diabetic macrosomia compared to normal pregnancies. However, there was no significant difference in the BW/PW ratio between nondiabetic macrosomia and normal pregnancies. This finding implied that the placenta from pregnancies with diabetic macrosomia failed to adapt their capacity for nutrient transfer, whereas, in isolated or nondiabetic macrosomia, the placenta maintains its efficiency in response to increased maternal nutritional supplies for the growing fetus.

The placental syncytioplasm and the fetal capillaries within the terminal villi function as a unit,<sup>22</sup> collectively referred to as the VSM. The VSM is a physical barrier between maternal and fetal blood.<sup>23</sup> A key function of the VSM is to maintain the exchange area and regulate the diffusion distance of fetomaternal surfaces.<sup>24</sup> In our study, we observed an increased thickness in the VSM and syncytial BM in placentas from pregnancies with diabetic macrosomia. This finding is consistent with previous studies that have reported thickened VSM and BM in placentas affected by GDM.<sup>25,26</sup> This

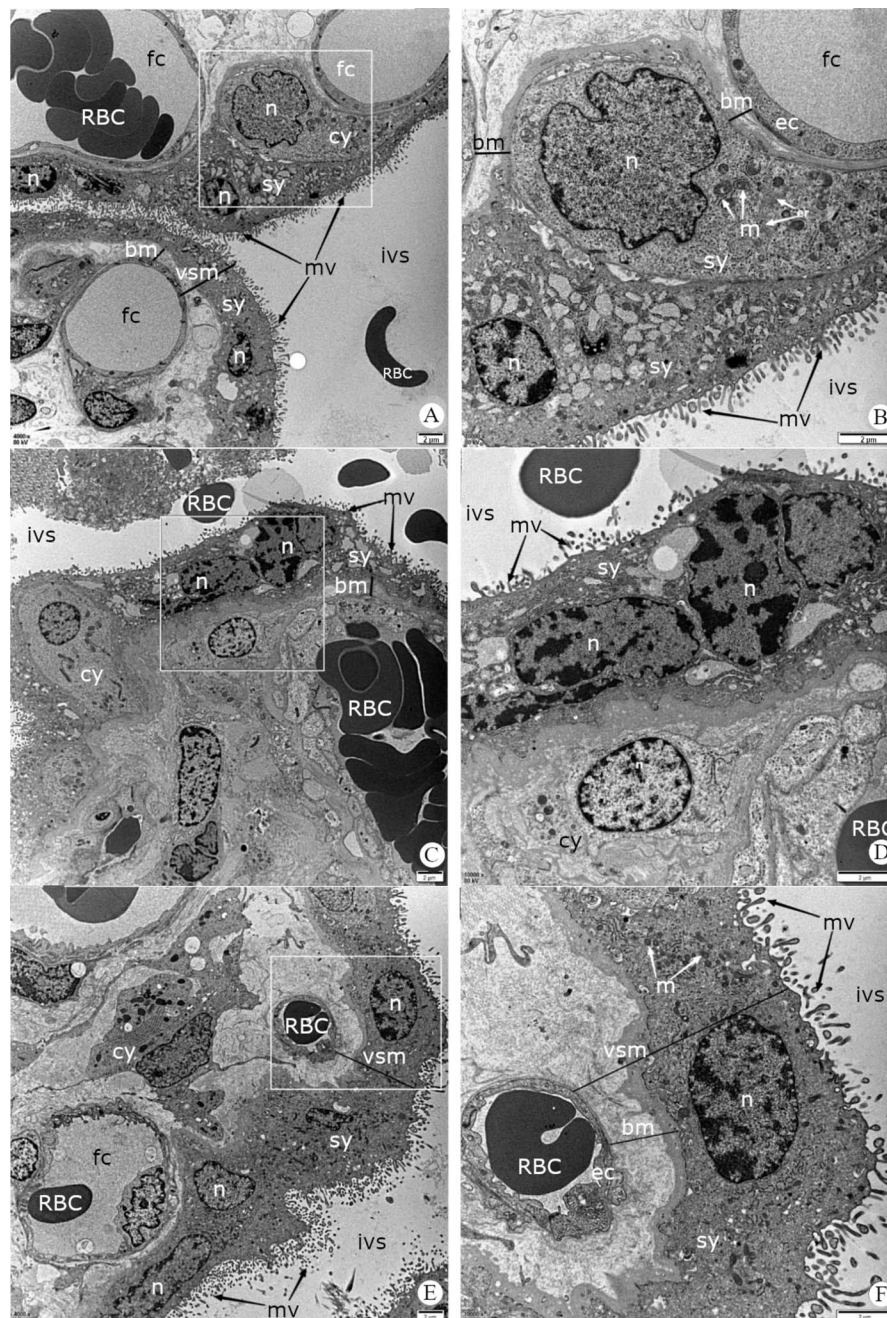


**Figure 1.** Ultrastructure of ultrathin section of human placenta from control group (A, B), macrosomia (C, D), and macrosomia with maternal gestational diabetes mellitus (E, F) observed by TEM. TEM images at  $\times 4000$  (A, C, E) and  $\times 10,000$  (B, D, F). A VSM with syncytiotrophoblasts and microvilli facing the intervillous space; maternal red blood cells visible. B Cytotrophoblastic cell with a large nucleus with fine disperse chromatin and few mitochondria covered by syncytium. C Nearly normal vasculo-syncytial membrane with microvilli and cytotrophoblasts separating syncytiotrophoblasts from fetal capillary. D Thick cytotrophoblast basement membrane with fiber bundles and few short-blunted microvilli. E Thick vasculo-syncytial membrane with detached microvilli. F Thick irregular vasculo-syncytial membrane with diminished distorted microvilli and vacuoles. bm: Basement membrane; cy: Cytotrophoblasts; fc: Fetal capillary; ivs: Intervillous space; m: Mitochondria; mv: Microvilli; n: Nucleus; RBC: Red blood cells; sy: Syncytiotrophoblasts; ec: Epithelial cell; TEM: Transmission electron microscopy; VSM: Vasculo-syncytial membrane.

increased thickness of the VSM in GDM pregnancies may be attributed to the accumulation of fibronectin, collagen, and polysaccharides resulting from impaired villous trophoblastic activities.<sup>27</sup> The syncytiotrophoblast is the key structure in the placenta responsible for nutrient sensing and allows the fetus to regulate its own growth by extracting nutrients

from the maternal blood.<sup>28</sup> Alteration of the thickness of this layer could cause disorders in nutrient-sensing pathways and may lead to fetal growth disorders such as macrosomia. For example, when the placenta is exposed to an excess of nutrients in gestational diabetes, an acceleration in fetal growth may be expected to occur via the activation of the



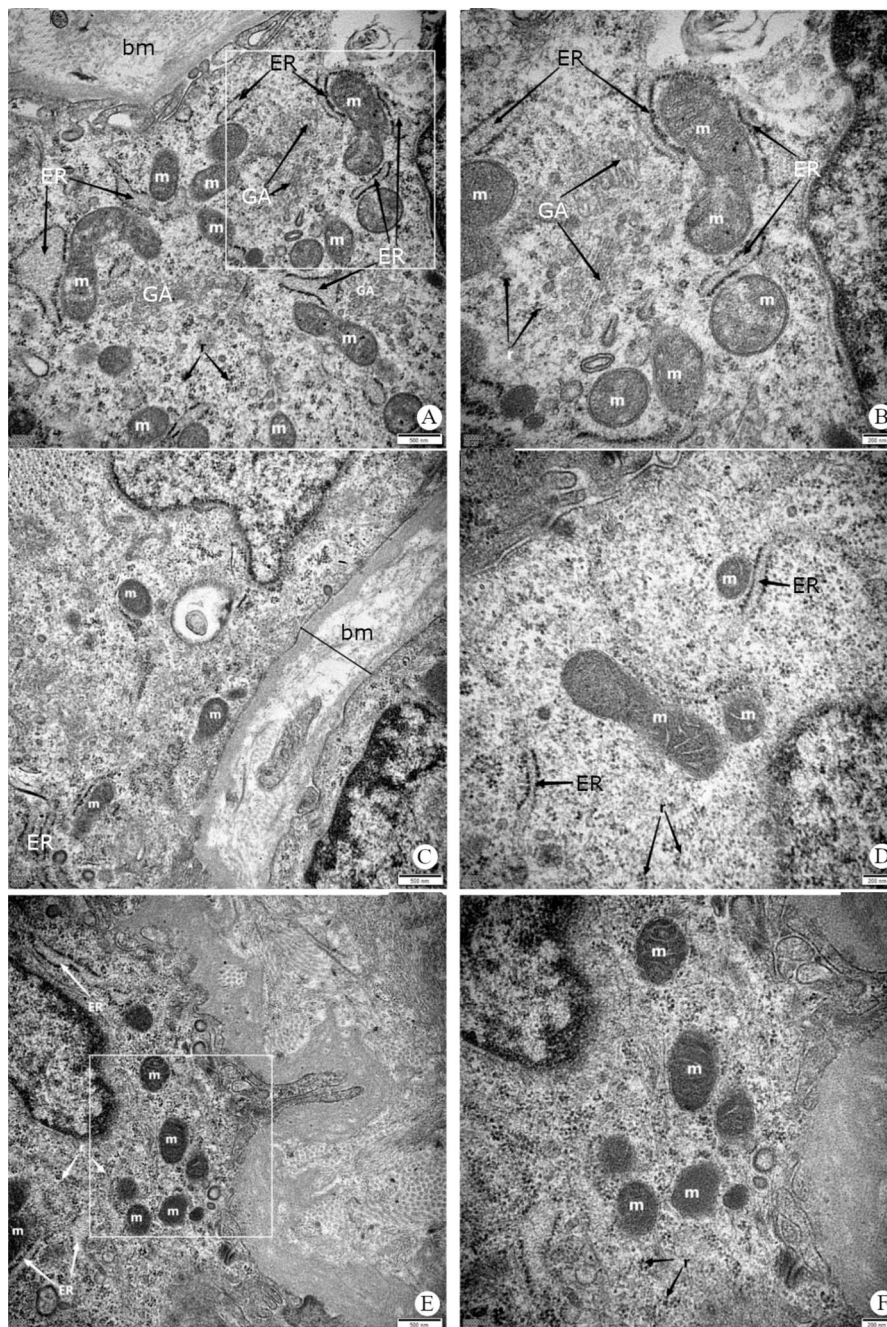


**Figure 2.** Ultrastructure of cytoplasmic organelles from control group (A, B), macrosomia (C, D), and macrosomia with maternal gestational diabetes mellitus (E, F) observed by TEM. TEM images are at different magnifications, including  $\times 30,000$  (A, C, E) and  $\times 50,000$  (B, D, F). A Cytotrophoblastic cell with granular cytoplasm, abundant mitochondria, and free ribosomes. B Round or oval mitochondria with clear cristae, rough ER, and Golgi apparatus in the control group. C Few mitochondria and rough ER in cytotrophoblastic cells. D Slightly swollen mitochondria with less clear cristae. E Cytotrophoblast with few distorted, swollen mitochondria. F Mitochondria with lost cristae and dilated ER. bm: Basement membrane; ER: Endoplasmic reticulum; GA: Golgi apparatus; m: Mitochondria; r: Ribosomes; TEM: Transmission electron microscopy.

mechanistic target of rapamycin (mTOR) signaling pathways.<sup>29</sup> Emerging evidence suggests that mTOR signaling has a role in regulating fetal growth; however, more studies should be performed following a vigorous and unanimous method for assessment to determine placental mTOR activity.<sup>30</sup> Thickening of the microvilli can potentially alter the transport capacity and efficiency of placental vasculature, leading to the reduced transport of nutrients and oxygen.

Such changes may contribute to fetal hypoxia and pose a significant risk to the fetus.

Using stereological comparison, we observed a significant decrease in the volume and surface density of microvilli in the placenta of diabetic macrosomia cases. The density of microvilli is associated with the degree of trophoblastic maturation.<sup>31</sup> Distorted microvilli or loss of microvilli has been reported in the terminal villi of placentas from women with



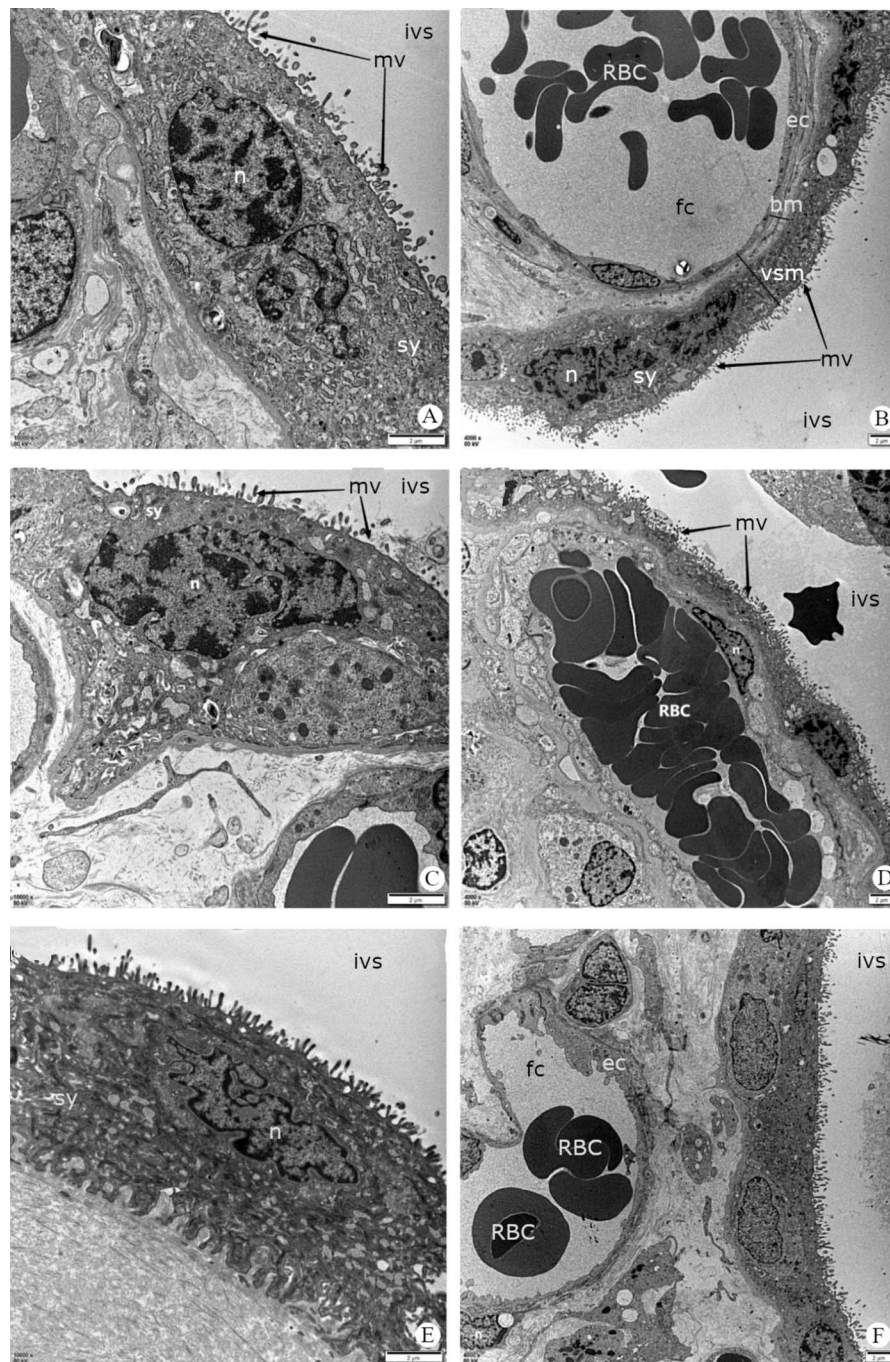


**Figure 3.** Ultrastructure of nucleus and fetal capillary from control group (A, B), macrosomia (C, D), and macrosomia with maternal gestational diabetes mellitus (E, F) observed by TEM. TEM images are at different magnifications, including  $\times 10,000$  (A, C, E) and  $\times 4000$  (B, D, F). A Large nucleus with fine dispersed chromatin. B Thin syncytial basement membrane in direct contact with endothelial cells of the fetal capillary, lined with simple squamous endothelial cells with flat nuclei. C Nearly normal condensed heterochromatic syncytial nuclei and regular nuclear membrane. D Fetal blood capillary with a smooth endothelial surface and red blood cells in its lumen. E Folded, edematous nuclear membrane with chromatin in dense peripheral clumps. F Irregular, split basement membrane with an irregular endothelial surface and narrow lumen. bm: Basement membrane; cy: Cytotrophoblasts; ec: Endothelial cells; fc: Fetal capillary; ivs: Intervillous space; mv: Microvilli; n: Nucleus; RBC: Red blood cells; sy: Syncytiotrophoblasts; TEM: Transmission electron microscopy; VSM: Vasculo-syncytial membrane.

eclampsia,<sup>32</sup> and a considerable reduction in apical microvilli density has been observed in small-for-gestational-age fetuses.<sup>33</sup> A decreased density of microvilli suggests a compromised exchange of nutrients, gases, and waste between the maternal and fetal circulatory systems. A significant

decrease in apical microvilli density has also been documented in placentas of individuals with uncontrolled DM.<sup>25</sup> A possible explanation for this change is that exposure to hypoxia in a diabetic environment contributes to decreased density of microvilli.<sup>34</sup> Such alteration would impact

**Table 3**

**Comparison of stereological parameters of microvilli under TEM examination in the three groups.**

Parameter	Control group ( <i>n</i> = 20)	Nondiabetic macrosomia group ( <i>n</i> = 20)	Diabetic macrosomia group ( <i>n</i> = 20)	<i>t</i>	<i>P</i>
Volume density (mm <sup>0</sup> )	0.461 ± 0.082	0.368 ± 0.074	0.324 ± 0.058	8.586	<0.001*
Surface density (mm <sup>-1</sup> )	0.047 ± 0.031	0.041 ± 0.018	0.030 ± 0.006	3.463	0.044†
Shape	0.534 ± 0.076	0.469 ± 0.058	0.411 ± 0.042	13.664	<0.001‡
Distribution	0.524 ± 0.039	0.618 ± 0.044	0.667 ± 0.056	17.095	<0.001§
Average thickness of syncytiotrophoblast BM (nm × 10 <sup>-3</sup> )	0.106 ± 0.015	0.163 ± 0.025	0.214 ± 0.031	36.309	<0.001§
Average thickness of fetal capillary BM (nm × 10 <sup>-3</sup> )	0.103 ± 0.026	0.172 ± 0.037	0.228 ± 0.057	15.824	<0.001§

Data are presented as mean ± standard deviation.

\*Volume density significantly differed between the control group and both the nondiabetic and diabetic macrosomia groups.

†Surface density significantly differed between the diabetic macrosomia group and both the control and nondiabetic groups.

‡Shape significantly differed between the control and diabetic macrosomia group.

§The three groups all showed significant differences from each other in the parameters of distribute, average thickness of syncytiotrophoblast BM, and average thickness of fetal capillary BM.

BM: Basement membrane; TEM: Transmission electron microscopy.

transplacental transfer, metabolism, and oxygen diffusion within the placenta.

TEM examination revealed swollen and distorted mitochondria and a dilated rough ER in the placenta of diabetic macrosomia, which aligns with findings from previous studies. Hyperglycemia and hypoxia associated with diabetes would cause profound syncytial damage, with mitochondria and the ER being particularly vulnerable to the effects of hyperglycemia.<sup>35</sup> The abnormal ultrastructure of mitochondria and the rough ER could impact the metabolic functions of the trophoblast. We also observed abnormalities in the vascular endothelium of the placenta from cases of diabetic macrosomia, including endothelial cell enlargement, thickening, and protrusion into the vascular lumen. The fetal capillary BM also exhibited abnormalities, such as increased thickness and splitting. These changes may be a response to oxidative stress induced by hyperglycemia. Furthermore, the above changes in placental mitochondria and vascular endothelium may cause endothelial dysfunction, which could induce preeclampsia. The common antidiabetic drug metformin is a prevention and treatment agent for hyperglycemia in pregnancy and preeclampsia, as it reduces the production of antiangiogenic factors, such as soluble vascular endothelial growth factor receptor- $\alpha$  and soluble endoglin, and improves endothelial dysfunction through targeting mitochondria.<sup>28</sup>

In summary, our study revealed significant alterations in the morphology and ultrastructure of terminal villi and apical microvilli in the human placenta complicated by GDM and macrosomia. However, the limited sample size of this study means further investigations and molecular experiments are needed to elucidate the underlying mechanisms of the observed changes. Exploring the pathways through which these ultrastructural alterations regulate the development and function of the placenta and the processes of transport, metabolism, and endocrine function is essential since this is a crucial step in developing new therapies for preventing and treating GDM-induced macrosomia.

**Acknowledgments**

We thank Miaomiao Song and Na Zhao for their assistance with sample collection, and to all the pregnant women who participated in this study.

**Funding**

This study was supported by the research grant from the Key Research and Development Program of Shaanxi Province (no. 2022SF-125, 2021ZDLSF02-14).

**Author Contributions**

Junxiang Wei and Yang Mi designed the overall study; Tianyu Dong collected the data and sample; Mingxia Chen did the electron microscope work; Junxiang Wei and Xiao Luo analyzed the data and interpreted the results. Junxiang Wei drafted the manuscript. Xiao Luo and Yang Mi critically revised the manuscript. All authors approved the final version of the manuscript.

**Conflicts of Interest**

None.

**Data Availability**

The datasets generated during and/or analyzed during the current study are available from the corresponding author on reasonable request.

**References**

[1] Sweeting A, Wong J, Murphy HR, et al. A clinical update on gestational diabetes mellitus. *Endocr Rev* 2022;43(5):763–793. doi: 10.1210/edrv/bnac003.

[2] Wang H, Li N, Chivese T, et al. IDF Diabetes Atlas: Estimation of Global and Regional Gestational Diabetes Mellitus Prevalence for 2021 by International Association of Diabetes in Pregnancy Study Group's Criteria. *Diabetes Res Clin Pract* 2022;183:109050. doi: 10.1016/j.diabres.2021.109050.

[3] Gao C, Sun X, Lu L, et al. Prevalence of gestational diabetes mellitus in mainland China: A systematic review and meta-analysis. *J Diabetes Investig* 2019;10(1):154–162. doi: 10.1111/jdi.12854.

[4] Kc K, Shakya S, Zhang H. Gestational diabetes mellitus and macrosomia: A literature review. *Ann Nutr Metab* 2015;66(Suppl 2):14–20. doi: 10.1159/000371628.

[5] Plows JF, Stanley JL, Baker PN, et al. The pathophysiology of gestational diabetes mellitus. *Int J Mol Sci* 2018;19(11):3342. doi: 10.3390/ijms19113342.

[6] Burton GJ, Fowden AL, Thornburg KL. Placental origins of chronic disease. *Physiol Rev* 2016;96(4):1509–1565. doi: 10.1152/physrev.00029.2015.



- [7] Gauster M, Desoye G, Tötsch M, et al. The placenta and gestational diabetes mellitus. *Curr Diab Rep* 2012;12(1):16–23. doi: 10.1007/s11892-011-0244-5.
- [8] Sandovici I, Hoelle K, Angiolini E, et al. Placental adaptations to the maternal-fetal environment: Implications for fetal growth and developmental programming. *Reprod Biomed Online* 2012;25(1):68–89. doi: 10.1016/j.rbmo.2012.03.017.
- [9] Sferruzzi-Perri AN, Lopez-Tello J, Salazar-Petres E. Placental adaptations supporting fetal growth during normal and adverse gestational environments. *Exp Physiol* 2023;108(3):371–397. doi: 10.1113/EP090442.
- [10] Kretschmer T, Turnwald EM, Janoschek R, et al. Maternal high fat diet-induced obesity affects trophoblast differentiation and placental function in mice†. *Biol Reprod* 2020;103(6):1260–1274. doi: 10.1093/biolre/iaaa166.
- [11] Stuart TJ, O'Neill K, Condon D, et al. Diet-induced obesity alters the maternal metabolome and early placenta transcriptome and decreases placenta vascularity in the mouse. *Biol Reprod* 2018;98(6):795–809. doi: 10.1093/biolre/iy010.
- [12] Nteeba J, Varberg KM, Scott RL, et al. Poorly controlled diabetes mellitus alters placental structure, efficiency, and plasticity. *BMJ Open Diabetes Res Care* 2020;8(1):e001243. doi: 10.1136/bmjdr-2020-001243.
- [13] Metzger BE, Gabbe SG, Persson B, et al. International association of diabetes and pregnancy study groups recommendations on the diagnosis and classification of hyperglycemia in pregnancy. *Diabetes Care* 2010;33(3):676–682. doi: 10.2337/dc09-1848.
- [14] Heidari Z, Sakharav N, Mahmoudzadeh-Sagheb H, et al. Stereological analysis of human placenta in cases of placenta previa in comparison with normally implanted controls. *J Reprod Infertil* 2015;16(2):90–95.
- [15] Madhuri K, Jyothi I. A study on placental morphology in gestational diabetes. *J Evid Based Med Healthc* 2017;4(2):71–75. doi: 10.18410/jebmh/2017/14.
- [16] Saini P, Pankaj JP, Jain A, et al. Effect of gestational diabetes mellitus on gross morphology of placenta: A comparative study. *Int J Anat Res* 2015;3(1):889–894. doi: 10.16965/ijar.2015.111.
- [17] Wallace JM, Horgan GW, Bhattacharya S. Placental weight and efficiency in relation to maternal body mass index and the risk of pregnancy complications in women delivering singleton babies. *Placenta* 2012;33(8):611–618. doi: 10.1016/j.placenta.2012.05.006.
- [18] Effendi M, Demers S, Giguère Y, et al. Association between first-trimester placental volume and birth weight. *Placenta* 2014;35(2):99–102. doi: 10.1016/j.placenta.2013.11.015.
- [19] Desoye G, Cervar-Zivkovic M. Diabetes mellitus, obesity, and the placenta. *Obstet Gynecol Clin North Am* 2020;47(1):65–79. doi: 10.1016/j.ogc.2019.11.001.
- [20] Kedziora SM, Obermayer B, Sugulle M, et al. Placental transcriptome profiling in subtypes of diabetic pregnancies is strongly confounded by fetal sex. *Int J Mol Sci* 2022;23(23):15388. doi: 10.3390/ijms232315388.
- [21] Hayward CE, Lean S, Sibley CP, et al. Placental adaptation: What can we learn from birthweight: Placental weight ratio? *Front Physiol* 2016;7:28. doi: 10.3389/fphys.2016.00028.
- [22] Aplin JD. Developmental cell biology of human villous trophoblast: Current research problems. *Int J Dev Biol* 2010;54(2–3):323–329. doi: 10.1387/ijdb.082759ja.
- [23] Mihiu CM, Suşman S, Rus Ciucă D, et al. Aspects of placental morphogenesis and angiogenesis. *Rom J Morphol Embryol* 2009;50(4):549–557.
- [24] Burton GJ, Charnock-Jones DS, Jauniaux E. Regulation of vascular growth and function in the human placenta. *Reproduction* 2009;138(6):895–902. doi: 10.1530/REP-09-0092.
- [25] Meng Q, Shao L, Luo X, et al. Ultrastructure of placenta of gravidas with gestational diabetes mellitus. *Obstet Gynecol Int* 2015;2015:283124. doi: 10.1155/2015/283124.
- [26] Abdelhalim NY, Shehata MH, Gadallah HN, et al. Morphological and ultrastructural changes in the placenta of the diabetic pregnant Egyptian women. *Acta Histochem* 2018;120(5):490–503. doi: 10.1016/j.acthis.2018.05.008.
- [27] Pietryga M, Biczysko W, Wender-Ozegowska E, et al. Ultrastructural examination of the placenta in pregnancy complicated by diabetes mellitus. *Ginek Pol* 2004;75(2):111–118.
- [28] Romero R, Erez O, Hüttemann M, et al. Metformin, the aspirin of the 21st century: Its role in gestational diabetes mellitus, prevention of preeclampsia and cancer, and the promotion of longevity. *Am J Obstet Gynecol* 2017;217(3):282–302. doi: 10.1016/j.ajog.2017.06.003.
- [29] Shang M, Wen Z. Increased placental IGF-1/mTOR activity in macrosomia born to women with gestational diabetes. *Diabetes Res Clin Pract* 2018;146:211–219. doi: 10.1016/j.diabres.2018.10.017.
- [30] Dong J, Shin N, Chen S, et al. Is there a definite relationship between placental mTOR signaling and fetal growth? *Biol Reprod* 2020;103(3):471–486. doi: 10.1093/biolre/iaaa070.
- [31] Biagini G, Vasi V, Pugnali A, et al. Morphological development of the human placenta in normal and complicated gestation: A quantitative and ultrastructural study. *Gynecol Obstet Invest* 1989;28(2):62–69. doi: 10.1159/000293516.
- [32] Salgado SS, Salgado MKR. Structural changes in pre-eclamptic and eclamptic placentas—an ultrastructural study. *J Coll Physicians Surg Pak* 2011;21(8):482–486.
- [33] Ansari T, Fenlon S, Pasha S, et al. Morphometric assessment of the oxygen diffusion conductance in placentae from pregnancies complicated by intra-uterine growth restriction. *Placenta* 2003;24(6):618–626. doi: 10.1016/s0143-4004(03)00044-4.
- [34] de Luca Brunori I, Battini L, Brunori E, et al. Placental barrier breakage in preeclampsia: Ultrastructural evidence. *Eur J Obstet Gynecol Reprod Biol* 2005;118(2):182–189. doi: 10.1016/j.ejogrb.2004.04.024.
- [35] Pagliarini DJ, Calvo SE, Chang B, et al. A mitochondrial protein compendium elucidates complex I disease biology. *Cell* 2008;134(1):112–123. doi: 10.1016/j.cell.2008.06.016.

Edited By Yang Pan

**How to cite this article:** Wei J, Dong T, Chen M, Luo X, Mi Y. Unique Ultrastructural Alterations in the Placenta Associated With Macrosomia Induced by Gestational Diabetes Mellitus. *Maternal Fetal Med* 2024;6(3):164–172. doi: 10.1097/FM9.0000000000000240.